

Supporting Information (SI)

An advanced green fused diazonium initiating substance

Chengchuang Li^a, Jie Tang^a, Guangbin Cheng^{*a}, Chuan Xiao^{*b} and Hongwei Yang^{*a}

a. School of Chemistry and Chemical Engineering, Nanjing University of Science and Technology, Xiaolingwei 200, Nanjing, Jiangsu, China.

*Corresponding author E-mail: hyang@njust.edu.cn (H. Yang), gcheng@njust.edu.cn (G. Cheng).

b. China Northern Industries Group Co., Ltd. (NORINCO GROUP), Beijing 100089, P. R. China

*Corresponding author E-mail: 47785121@qq.com (C. Xiao).

Table of Contents

1. Experimental sections	1
2. Computational details	2
3. Crystallographic data	4
4. Spectra of compounds	6
5. DSC and TG of compounds	13
6. Computations for stabilities	13
7. References	16

1. Experimental sections

General methods

¹H and ¹³C NMR spectra were recorded on 500 MHz (Bruker AVANCE 500) nuclear magnetic resonance spectrometers operating at 500 and 126 MHz, respectively, by using DMSO-d₆ as the solvent and locking solvent unless otherwise stated. Chemical shifts in ¹H and ¹³C NMR spectra are reported relative to DMSO. DSC was performed in closed Al containers with a nitrogen flow of 30 mL min⁻¹ on an STD-Q600 instrument. Infrared (IR) spectra were recorded on a Perkin-Elmer Spectrum BX FT-IR equipped with an ATR unit at 25 °C. Impact sensitivity and friction sensitivity of samples are measured by using the standard BAM methods.

Synthesis

2-(amino(4-amino-1,2,5-oxadiazol-3-yl)methyl)malononitrile (**2**)

To a mixture of 4-amino-1,2,5-oxadiazole-3-carbonitrile (**1**) (5.00 g, 45.0 mmol) was suspended in 0.9 ml triethylamine and 60.0 ml methanol. A solution of malononitrile (2.00 g, 30.0 mmol) in distilled water (5.0 ml) was added dropwise at 0 °C. After the addition, the reaction mixture was stirred at room temperature for 6 h. To this solution was added (dropwise) the 37% HCl (0.5 ml). The solvent was spun dry under reduced pressure to give 7.86 g (98.2%) of compound **2** as a white solid. ¹H NMR (500 MHz, DMSO-d₆): δ = 6.62 (s), 9.30 (s) ppm. ¹³C NMR (126 MHz, DMSO-d₆): δ = 52.98, 114.52, 115.25, 142.19, 155.25, 158.02 ppm. ¹⁵N NMR (50.7 MHz, DMSO-d₆): δ = -338.41, 330.87, -118.13, -109.51, -15.71, 34.75 ppm.

, 142.19, 155.25, 158.02 ppm.

5-amino-3-(4-amino-1,2,5-oxadiazol-3-yl)-1H-pyrazole-4-carbonitrile (**3**)

To a mixture of **2** (1.78 g, 10.0 mmol) was suspended in 20.0 ml ethanol and 1.0 ml (20.0 mmol) hydrazine hydrate. The mixture was heated to 30 °C and stir for 3 hours. The precipitate was filtered and washed with water, and then dried in air to obtain 1.73 g (91.0%) of compound **3** as a yellow solid. ¹H NMR (500 MHz, DMSO-d₆): δ = 6.33 (s), 6.80 (s) ppm. ¹³C NMR (126 MHz, DMSO-d₆): δ = 71.21, 114.62, 139.91, 140.24, 154.92, 155.27 ppm. ¹⁵N NMR (50.7 MHz, DMSO-d₆): δ = -336.36, -326.81, -195.00, -114.02, -104.08, -20.79, 22.49 ppm.

3-amino-3-(4-amino-1,2,5-oxadiazol-3-yl)-2-(1H-tetrazol-5-yl)propanenitrile (**4**)

To a suspension of compound **2** (0.89 g, 5 mmol) in 30 mL water, 0.34 g NaN_3 was added in small portions with stirring at 0 °C. The mixture was then heated to 90 °C and reacted for 10 h. The precipitates were filtered, washed with water, and dried in air as a brown solid with a yield of 80.0% (0.88 g). ^1H NMR (500 MHz, DMSO- d_6): δ = 5.75 (s), 9.71 (br) ppm. ^{13}C NMR (126 MHz, DMSO- d_6): δ = 90.30, 139.75, 142.14, 153.36, 1154.53, 160.09 ppm. ^{15}N NMR (50.7 MHz, DMSO- d_6): δ = -338.26, -337.25, -180.11, -118.68, -98.09, -25.88, -15.39, 6.29, 35.16 ppm.

(E)-N-(6-amino-[1,2,5]oxadiazolo[3,4-*b*]pyrazolo[5,4-*d*]pyridin-5(4H)-ylidene)nitramide (**OPPD**)

To a mixture of trifluoroacetic acid (0.4 mL), trifluoroacetic anhydride (0.4 mL) and 100% nitric acid (2.0 mL) was added compound **3** (0.19 g, 1.0 mmol) at 0 °C. After being stirred for 24 h at room temperature, the solution was poured into ice. The precipitate was collected through filtration, washed with water to obtain 0.21 g (85.0%) of compound OPPD as a white solid. ^{13}C NMR (126 MHz, DMSO- d_6): δ = 135.24, 140.13, 143.83, 149.23, 152.31, 152.37 ppm. IR (KBr): $\tilde{\nu}$ 3453, 3345, 3289, 3241, 3029, 2221, 2219, 1690, 1644, 1610, 1590, 1420, 1412, 1137, 976, 879, 651 cm^{-1} . Elemental analysis for $\text{C}_6\text{HN}_9\text{O}_3$ (247.13): calcd C, 29.16; H, 0.41; N, 51.01%. Found: C 29.12, H 0.43, N 51.03%.

5-amino-6-azido-[3',4':5,6]pyrido[4,3-*d*][1,2,3]triazine[1,2,5]oxadiazolo-8-oxide (**OPTA**)

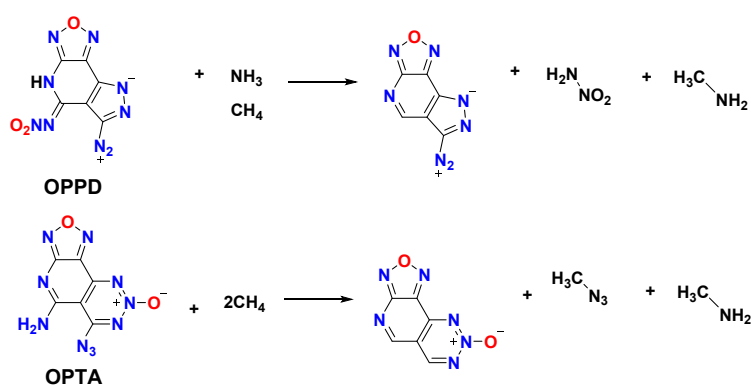
To a mixture of trifluoroacetic acid (0.4 mL), trifluoroacetic anhydride (0.4 mL) and 100% nitric acid (2.0 mL) was added compound **4** (0.22 g, 1.0 mmol) at 0 °C. After being stirred for 24 h at 25 °C, the solution was poured into ice. The precipitate was collected through filtration to obtain 0.15 g (60.7%) of compound OPTA as a yellow solid. ^1H NMR (500 MHz, DMSO- d_6): δ = 5.43 (s), ppm. ^{13}C NMR (126 MHz, DMSO- d_6): δ = 140.46, 143.55, 156.81, 159.69, 160.66, 161.37. IR (KBr): $\tilde{\nu}$ 3447, 3340, 3023, 2245, 2207, 2155, 1690, 1591, 1539, 1420, 1340, 1209, 877, 897, 741, 687, 540 cm^{-1} . Elemental analysis for $\text{C}_6\text{H}_2\text{N}_{10}\text{O}_2$ (246.15): calcd C, 29.28; H, 0.82; N, 56.90%. Found: C 29.24, H 0.81, N 56.95%.

2. Computational details.

Computations were performed by using the Gaussian09 suite of programs [1]. The elementary geometric optimization and the frequency analysis were performed at the level of the Becke three parameter, Lee-Yan-Parr (B3LYP) functional with the 6-311+G** basis set [2-4]. All of the optimized structures were characterized to be local

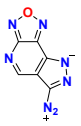

energy minima on the potential surface without any imaginary frequencies. Atomization energies were calculated by the CBS-4M [5]. All the optimized structures were characterized to be true local energy minima on the potential-energy surface without imaginary frequencies.

The predictions of heats of formation (HOF) of compounds used the hybrid DFTB3LYP methods with the 6-311+G** basis set through designed isodesmic reactions. The isodesmic reaction processes, that is, the number of each kind of formal bond is conserved, were used with the application of the bond separation reaction (BSR) rules. The molecule was broken down into a set of two heavy-atom molecules containing the same component bonds. The isodesmic reactions used to derive the HOF shown in Scheme S1.



Scheme S1. The isodesmic reactions for calculating heat of formation.

Table S1. Calculated zero-point energy (ZPE), thermal correction to enthalpy (HT), total energy (E0) and heats of formation (HOF)

Compound	E ₀ / a. u	ZPE / kJ mol ⁻¹	ΔH _T / kJ mol ⁻¹	HOF/kJ mol ⁻¹
OPPD	-947.603196	259.04	36.86	1069.701
OPTA	-927.776332	290.59	37.73	1076.082
	-687.543989	178.26	26.95	945.0035
	-708.749632	165.62	34.27	689.25
CH ₄	-40.539622	117.6	10.04	-74.6
NH ₂ NO ₂	-261.124817	98.79	12.39	-3.9
CH ₃ N ₃	-204.15	126.22	14.41	302
CH ₃ NH ₂	-95.8938402	160.78	11.64	-22.5
NH ₃	-56.5669848	86.27	10.05	45.9

3. Crystallographic data

Table S2. Crystallographic data for OPPD and OPTA.

Crystal	OPPD	OPTA
CCDC number	2357111	2323657
Empirical Formula	C ₆ H ₂ N ₉ O ₃	C ₆ H ₂ N ₁₀ O ₂
Formula weight	248.17	246.18
Temperature [K]	193.0	193.0
Crystal system	orthorhombic	monoclinic
Space group	Pna2 ₁	P2 ₁ /c
<i>a</i> /Å	18.4623(6)	6.8098(2)
<i>b</i> /Å	9.1563(4)	6.1710(2)
<i>c</i> /Å	5.3802(2)	20.8098(7)
α /°	90	90
β /°	90	91.748(2)
γ /°	90	90
Cell volume (Å ³)	909.5(6)	874.09(5)
Formula Z	4	4
Density (g cm ⁻³)	1.805	1.871
μ (mm ⁻¹)	1.323	1.317
F (000)	496.0	496.0
Crystal Size (mm ³)	0.13×0.12×0.1	0.13×0.11×0.1
2 θ range for data collection (°)	9.58 to 16.396	8.502 to 136.088
Index ranges	-20 ≤ <i>h</i> ≤ 22, -11 ≤ <i>k</i> ≤ 10, -6 ≤ <i>l</i> ≤ 5	-8 ≤ <i>h</i> ≤ 8, -6 ≤ <i>k</i> ≤ 7 -25 ≤ <i>l</i> ≤ 24
Reflections collected	7335 1559	7841 3006
Independent reflections	[R _{int} = 0.0879, R _{sigma} = 0.0876]	[R _{int} = 0.0529, R _{sigma} = 0.0362]
Data/restraints/parameters	1559/2/163	1580/1/163
Goodness-of-fit on F ²	1.111	1.074
Final R indexes [I ≥ 2 σ (I)]	R ₁ = 0.0436, wR ₂ = 0.1113	R ₁ = 0.0343, wR ₂ = 0.0888
Final R indexes [all data]	R ₁ = 0.0522,	R ₁ = 0.0461,

$$wR_2 = 0.1161$$

$$wR_2 = 0.0945$$

Table S3. Torsion angles for OPPD.

Parameter	Bond angles (Å)	Parameter	Bond angles (Å)
N5-O1-N4-C6	-0.6(5)	N7-N6-C5-C4	-1.2(5)
N4-O1-N5-C5	-0.4(5)	N7-N6-C3-N1	177.0(4)
N1-N2-C3-N3	-0.3(6)	N7-C1-C2-C3	177.5(4)
N1-N2-C3-C2	179.1(3)	N7-C1-C2-C4	-1.4(4)
O2-N1-N2-C3	5.1(5)	C2-C4-C5-N5	-179.7(4)
C6-N3-C3-N2	179.5(4)	C2-C4-C5-C6	-1.5(5)
C6-N3-C3-C2	0.1(6)	C3-C2-C4-C6	-177.5(4)
N4-N6-N7-C1	0.2(4)	C1-C2-C4-C5	-177.0(3)

Table S4. Hydrogen bonds for OPPD.

D-H...A	d(D-H)/ Å	d(H...A)/ Å	d(D...A)/ Å	<(DHA)/ °
N3-H3...O2	0.8800	2.0000	2.587(5)	122.00
N3-H3...O3	0.8800	2.2700	3.015(5)	142.00

Table S5. Torsion angles for OPTA.

Parameter	Bond angles (Å)	Parameter	Bond angles (Å)
N4-O1-N3-C2	0.60(18)	N7-N6-C3-C4	2.1(3)
N3-O1-N4-C1	-0.54(18)	C1-N5-C5-N12	175.62(16)
O1-N3-C2-C1	-0.41(19)	C1-N5-C5-C4	-3.0 (2)
O1-N3-C2-C3	178.04(18)	C3-N6-N7-O2	-1178.89(14)
O1-N4-C1-N5	179.76(16)	C3-N6-N7-N8	0.9(2)
O1-N4-C1-C2	0.27(19)	C1-C2-C3-N6	-179.34(16)
N7-N6-C3-C2	-177.55(15)	C1-C2-C3-C4	1.0(2)

Table S6. Hydrogen bonds for OPTA.

D-H...A	d(D-H)/ Å	d(H...A)/ Å	d(D...A)/ Å	<(DHA)/ °
---------	-----------	-------------	-------------	-----------

D-H...A	d(D-H)/ Å	d(H...A)/ Å	d(D...A)/ Å	<(DHA)/ °
N12-H12A...N5	0.8800	2.1300	3.002(2)	172.00
N12-H12B...N9	0.8800	2.0600	2.738(2)	133.00

4. Spectra of compounds

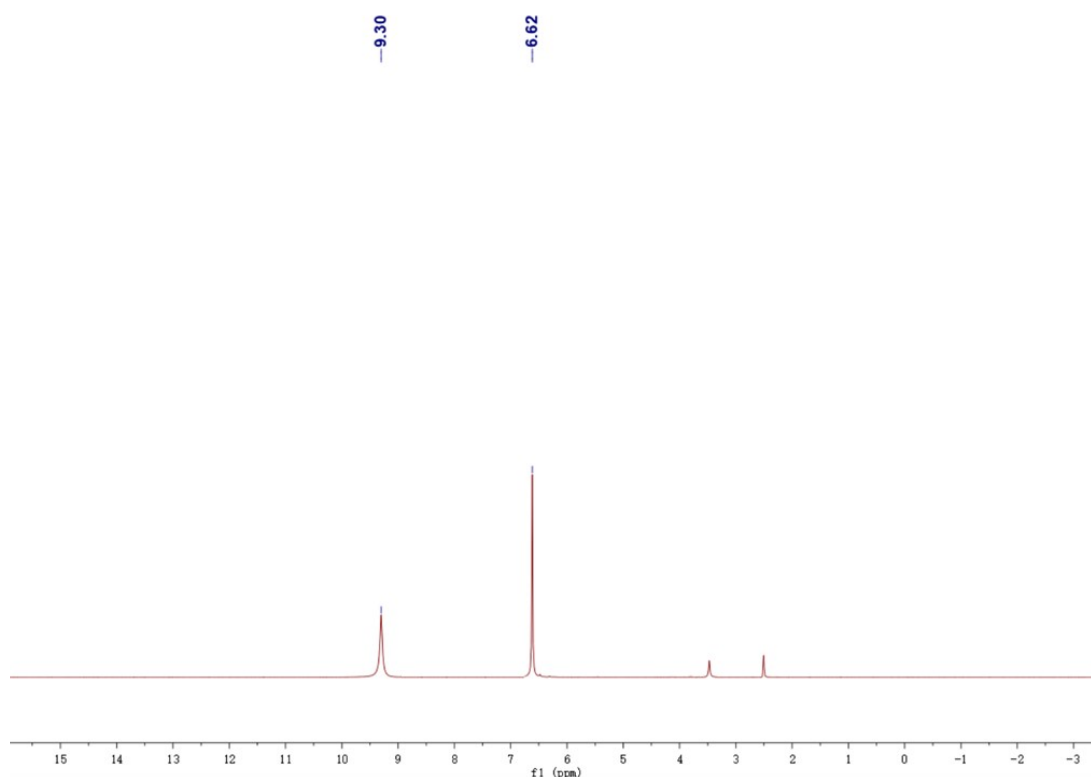


Figure S1. ¹H NMR spectrum in DMSO-d₆ for **2**.

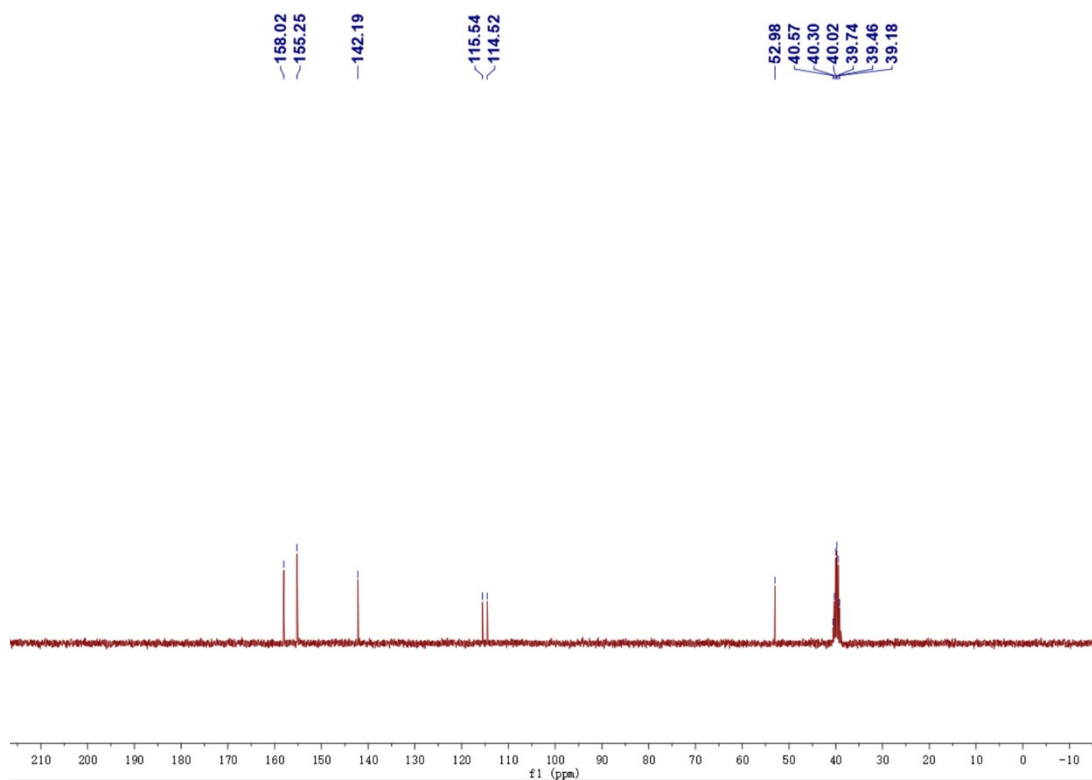


Figure S2. ^{13}C NMR spectrum in DMSO- d_6 for **2**.

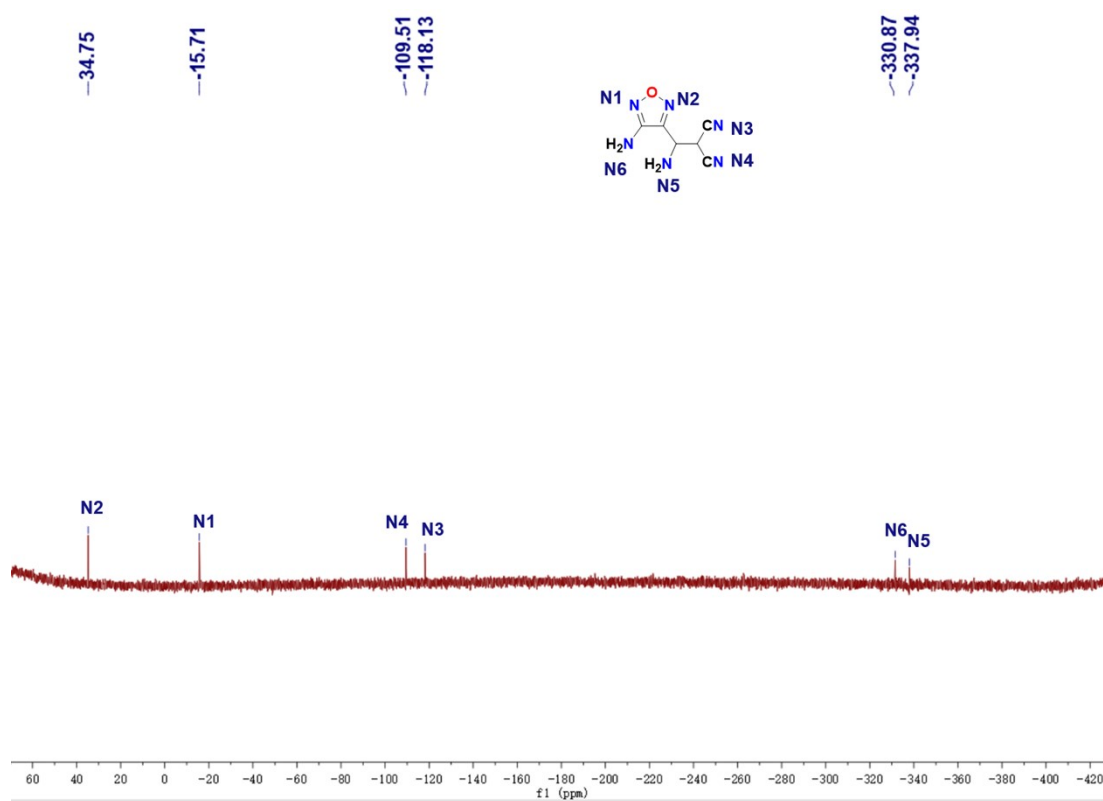


Figure S3. ^{15}N NMR spectrum in DMSO- d_6 for **2**.

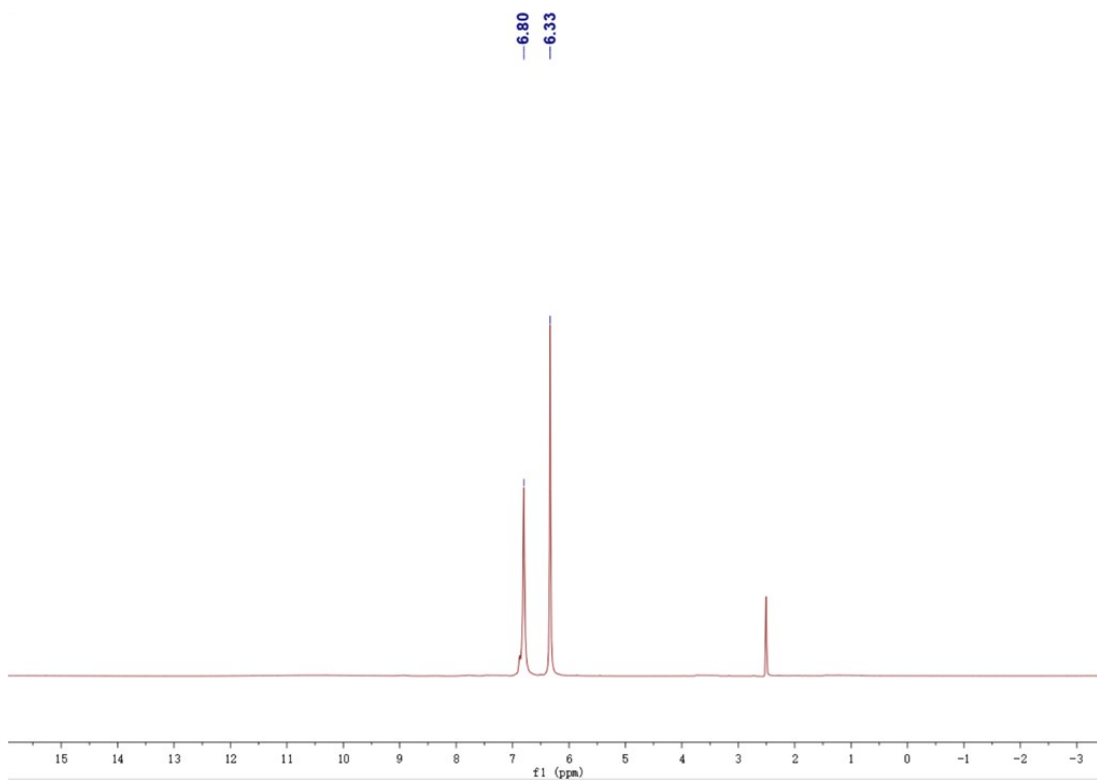


Figure S4. ^1H NMR spectrum in DMSO-d_6 for **3**.

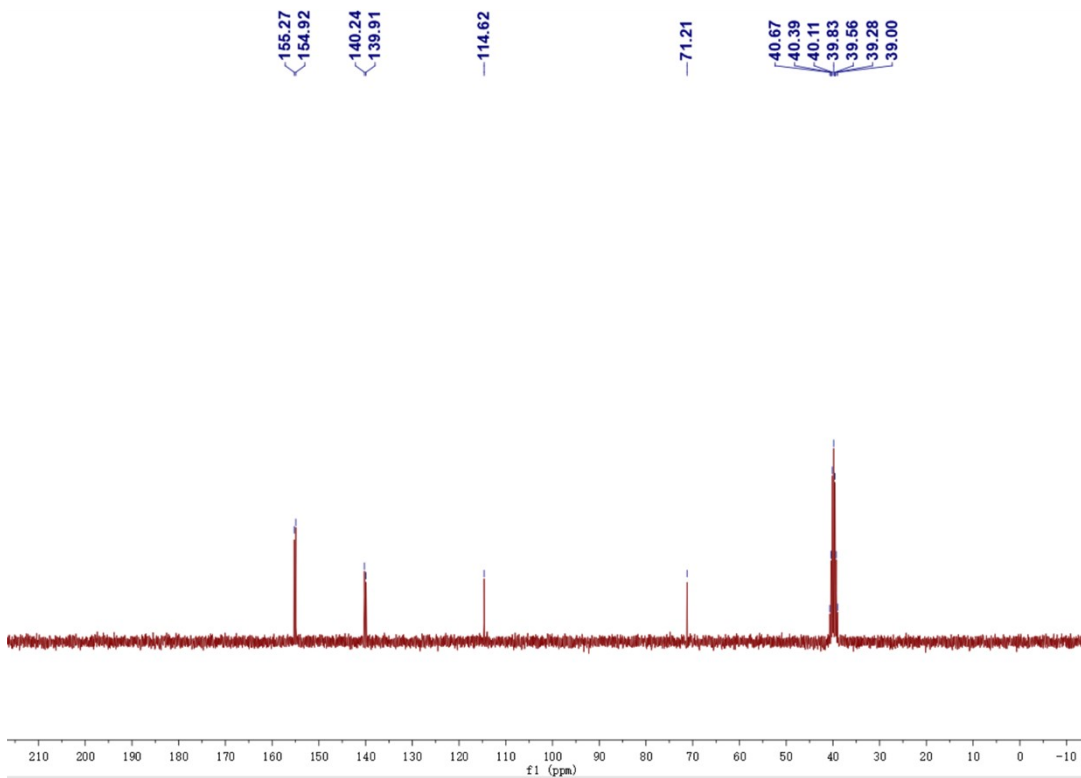


Figure S5. ^{13}C NMR spectrum in DMSO-d_6 for **3**.

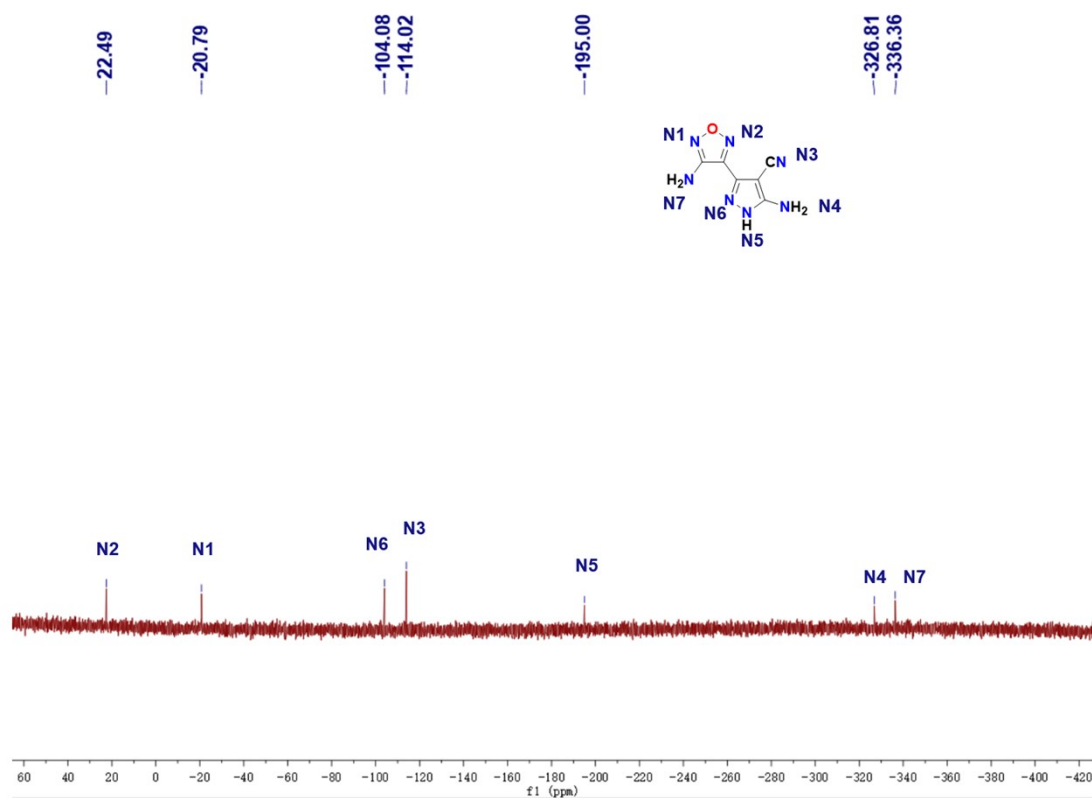


Figure S6. ¹⁵N NMR spectrum in DMSO-d₆ for **3**.

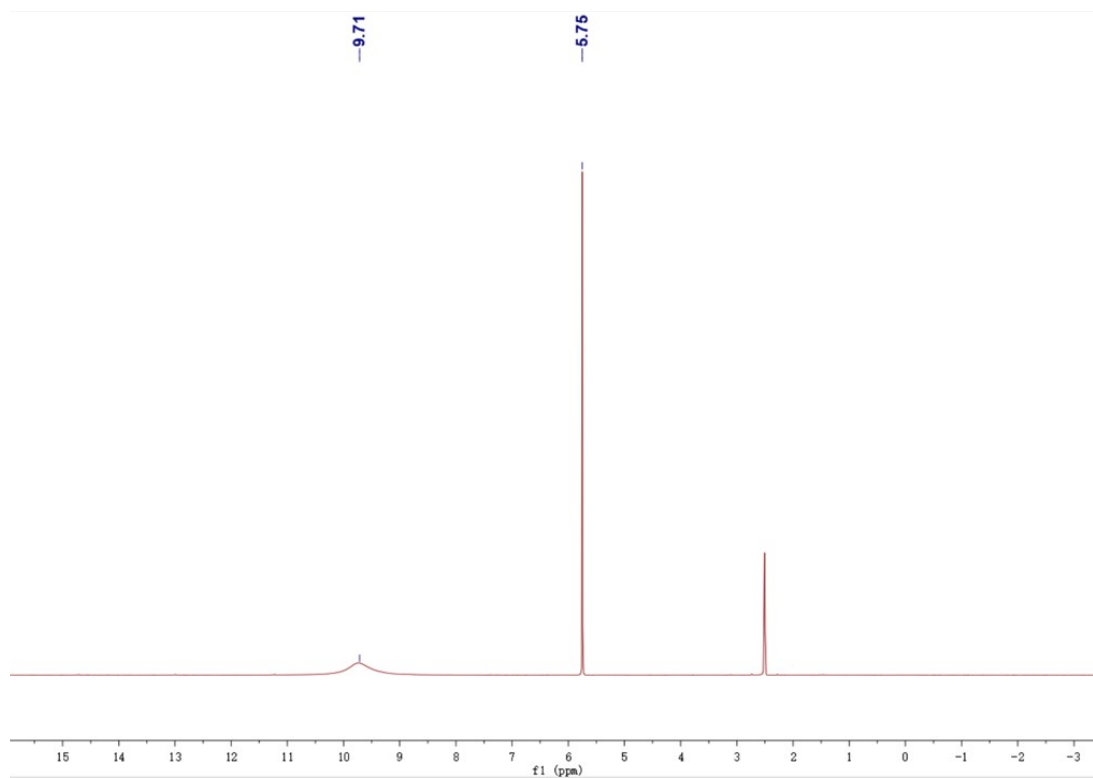


Figure S7. ^1H NMR spectrum in DMSO-d₆ for 4.

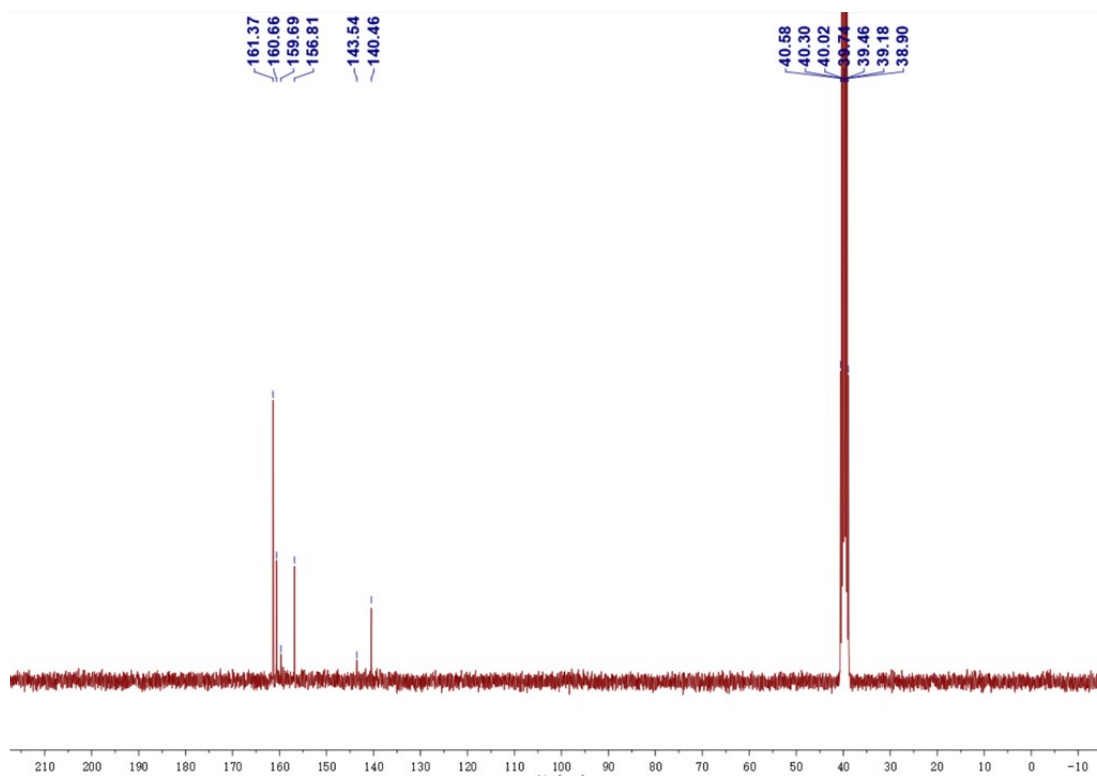


Figure S8. ^{13}C NMR spectrum in DMSO-d₆ for 4.

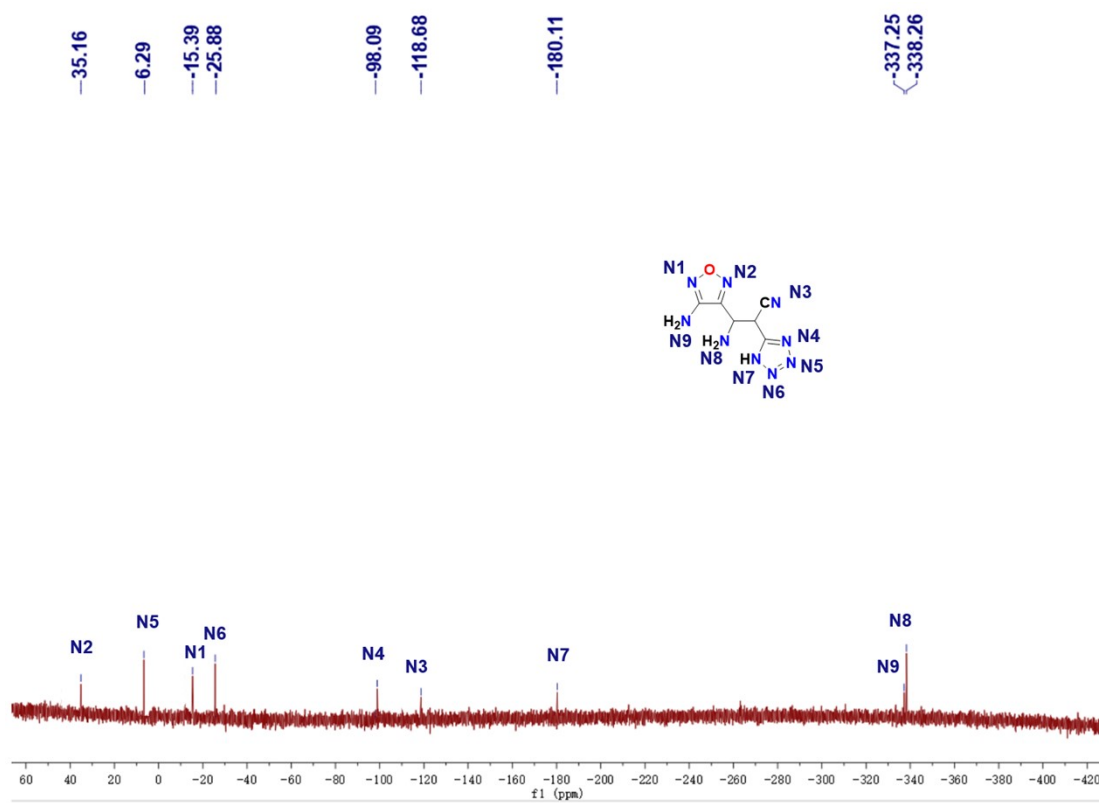


Figure S9. ^{15}C NMR spectrum in DMSO-d6 for **4**.

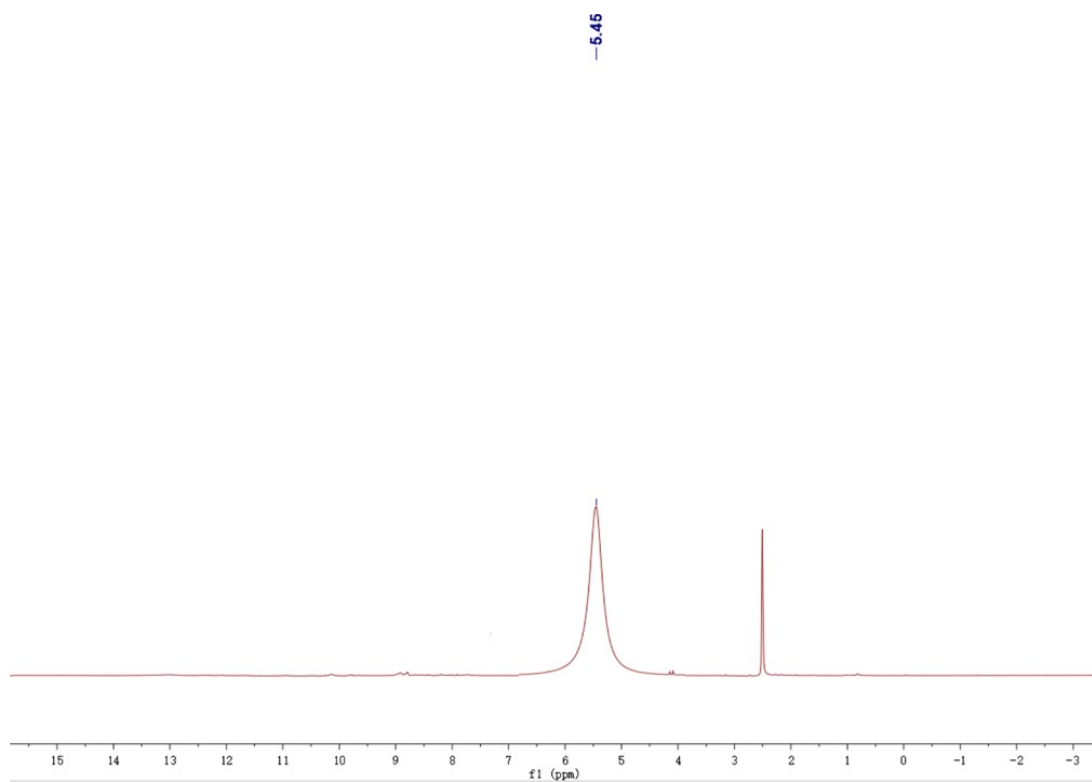


Figure S10. ^1H NMR spectrum in DMSO-d6 for OPTA.

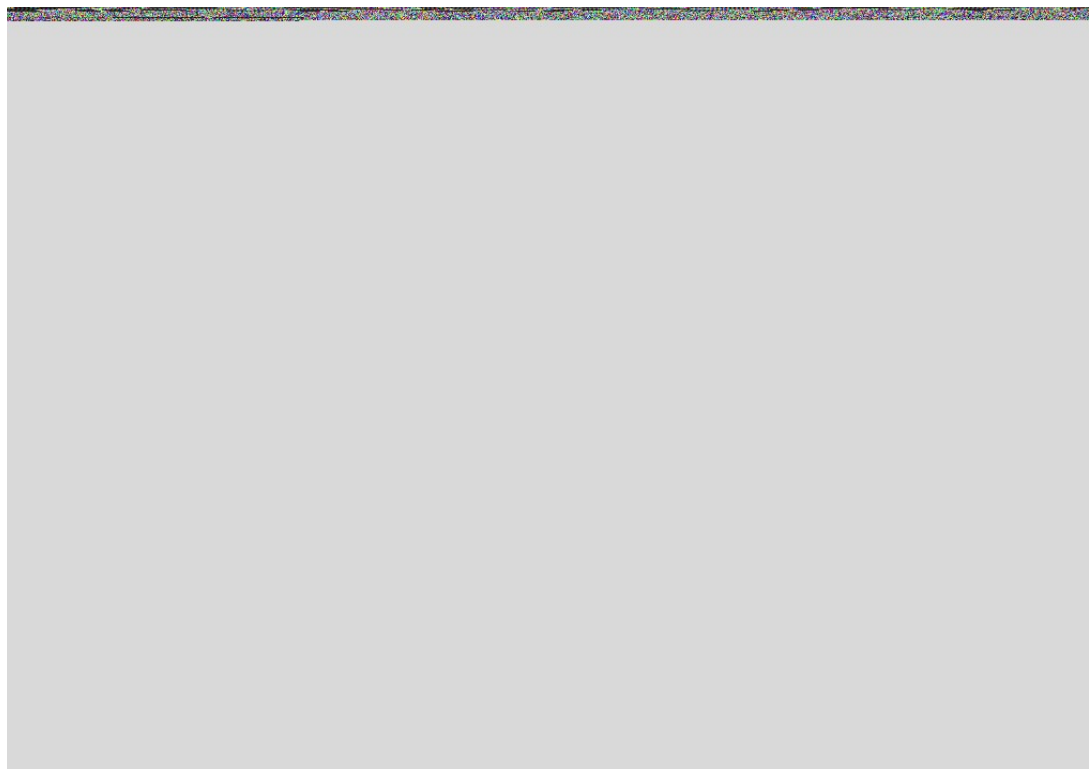


Figure S11. ^{13}C NMR spectrum in DMSO- d_6 for OPTA.

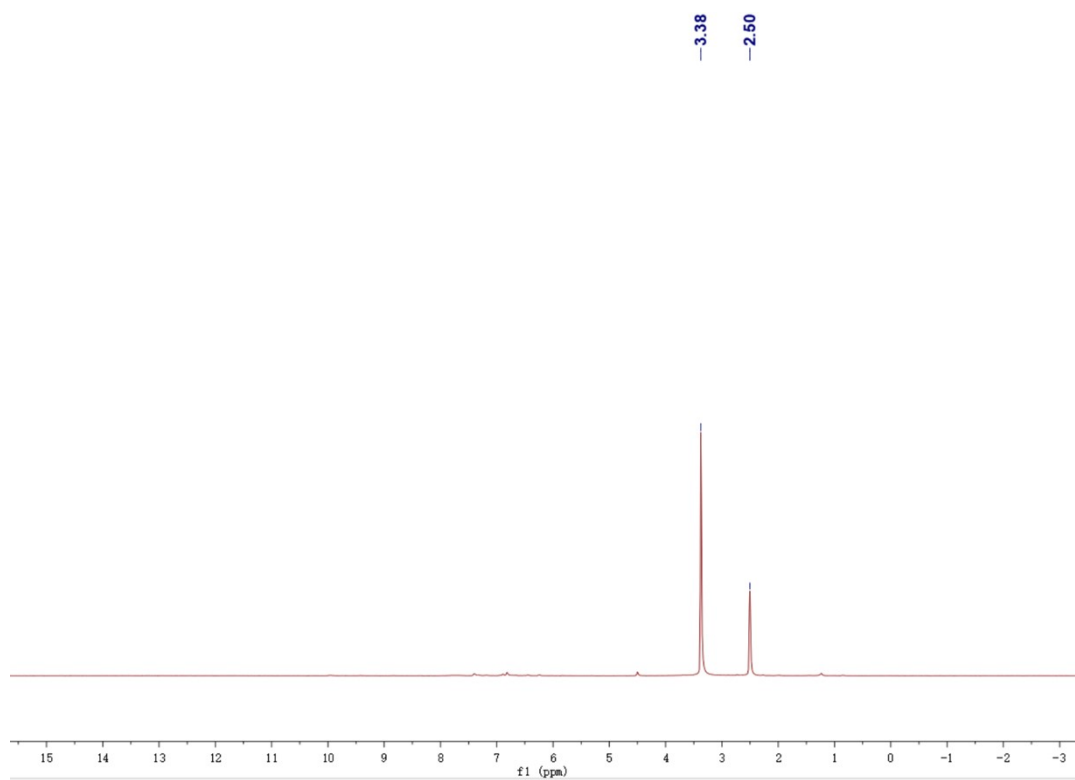


Figure S12. ^1H NMR spectrum in DMSO- d_6 for OPPD.

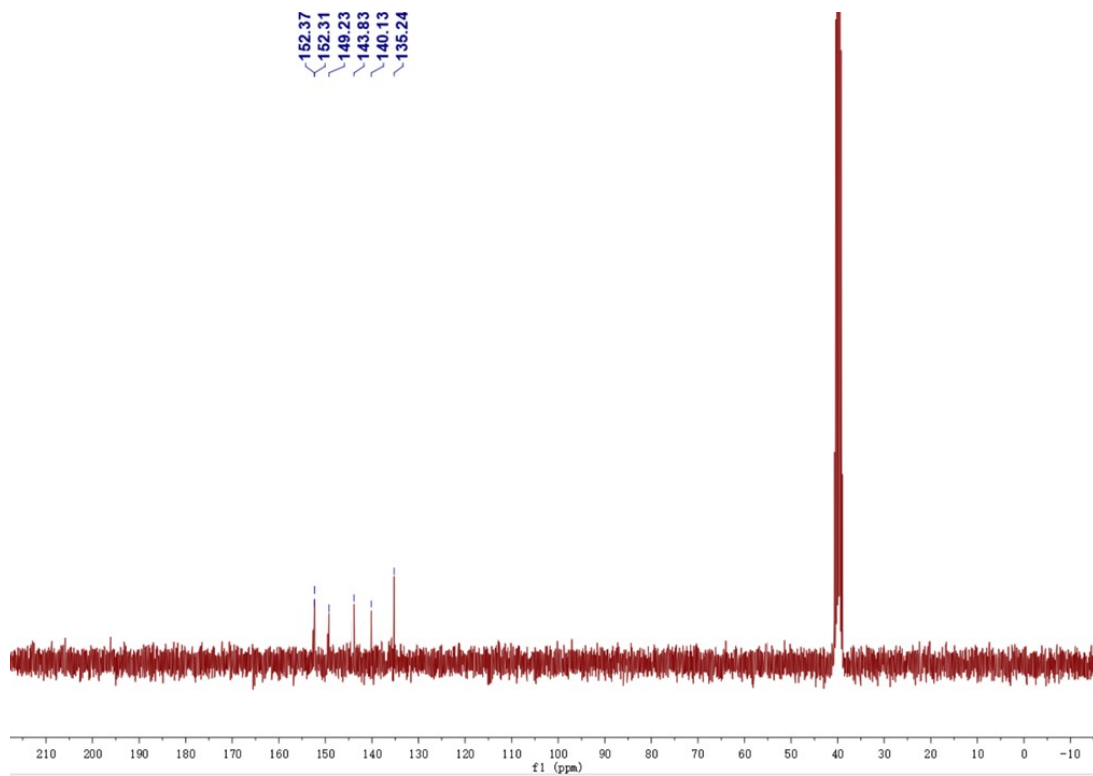


Figure S13. ^{13}C NMR spectrum in DMSO- d_6 for OPPD.

5. DSC and TG of compounds

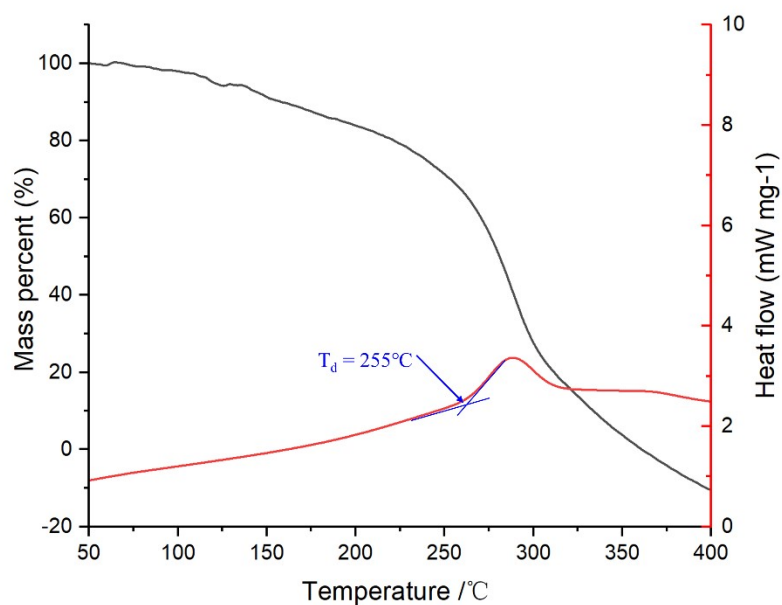


Figure S11 TG and DSC of OPTA (10K/min).

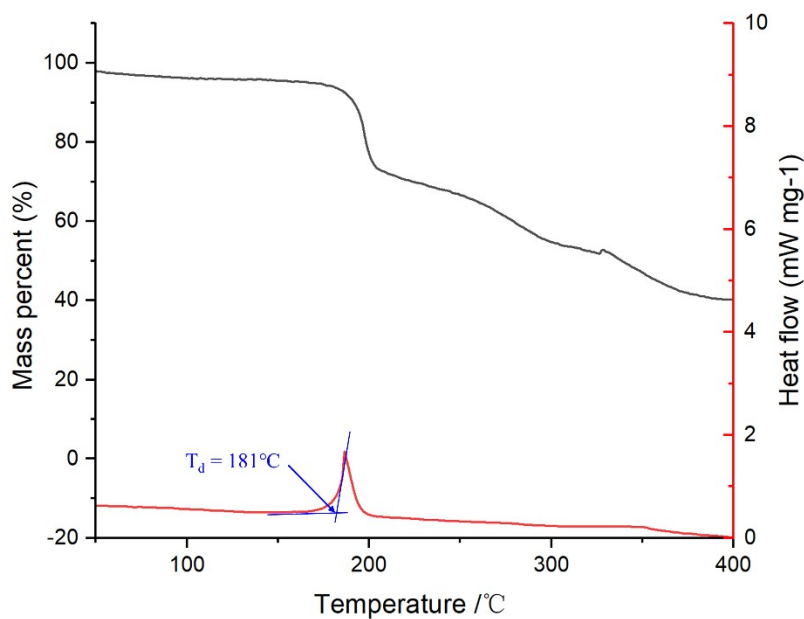


Figure S12 TG and DSC of OPPD (10K/min).

6. Computations for stabilities

Different from the previous reported diazoniums and azido compounds with extremely high sensitivity, compounds OPTA and OPPD possess suitable sensitivity as the primary explosive, which may be caused by the multi ring coplanar structure with a large conjugated system and cyclic strain energy [6-8]. To obtain additional

understanding of the great molecular stability and low mechanical sensitivity of OPTA and OPPD, a two-dimensional fingerprint analysis based on a Hirshfeld surface was utilized (Figure S13) [6-8]. Strong hydrogen bonds, such as those found in O-H and N-H interactions, are indicated by the red patches on the Hirshfeld surfaces (Figures S13a and S13c). According to Figure 5, the percentages of O-H and N-H hydrogen bond interactions in OPTA and OPPD are 20.2% and 12.0%, respectively. Strong intermolecular π - π interactions in the crystals of OPTA and OPPD are confirmed by the comparatively large fraction of interactions (e.g., N...O and N...N interactions) belonging to interlayer atomic contacts (51.3 % and 59.0 %, respectively). These weak interactions may contribute to increasing crystal density and decreasing IS and FS values.

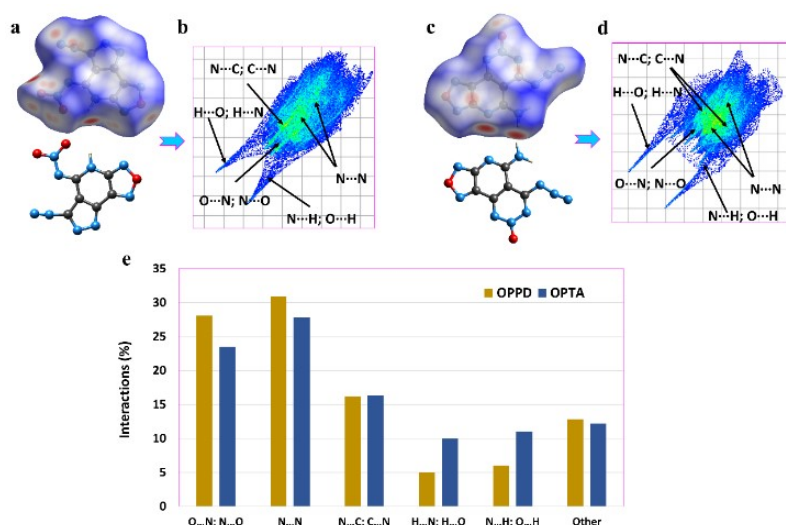


Figure S13. Hirshfeld surfaces of molecules OPTA (a) and OPPD (c). Two-dimensional fingerprint plots in crystal stacking OPPD (b) and OPTA (d). In images (e), the percentage contributions of the individual atomic contacts to the Hirshfeld surface were shown.

In general, there is a close relationship between the thermal stability and aromaticity of energetic materials [9,10]. This study evaluated the aromaticity of fused tricyclic compounds using the Local Orbital Locator- π (LOL- π) and multicenter bond ordering prediction models [10,11]. Figure S14c and S14f reveal the results of the multicenter bond orders of N-heterocyclic ring of the fused [5,6,6], [5,6,5]-tricyclic energetic molecule OPTA and OPPD. The multicenter bond order of fused ring and hexagonal ring in OPTA (0.5269; 0.4650) is higher than that in OPPD (0.5252; 0.4169), indicating that the better aromaticity. In addition to comparing with the domains of multicenter bond ordering analysis, the LOL- π may also be used to characterize the aromaticity of N-heterocyclic rings. The LOL-isosurface maps in Figure S14a to S14d show that the distribution of π -electrons dispersed on the fused-ring by OPTA is more continuous than that of the OPPD, indicating stronger π - electron conjugation. In addition, compared to the fused [5,6,6]-tricycle, the bright area on the fused [5,6,5]-tricycle in the LOL- π diagram is larger, indicating a larger distribution of π - electrons, which is consistent with the analysis of the LOL-isosurface maps analysis. In conclusion, the

thermal stability of OPTA ($T_d = 255\text{ }^\circ\text{C}$) is superior to those of OPPD ($T_d = 181\text{ }^\circ\text{C}$) can be supported from these predictive models.

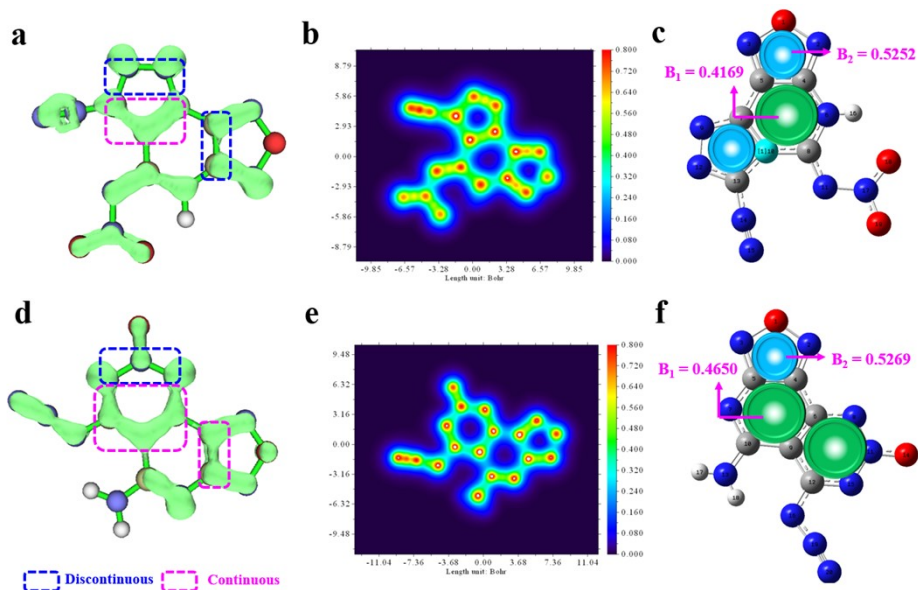


Figure S14. The localized orbital locator- π (LOL- π) isosurface graphs for OPTA (a) and OPPD (d); localized orbital locator- π diagrams of compounds OPTA (b) and OPPD (e) above the XY plane; the multicenter bond orders analysis for OPTA (c) and OPPD (f) (B_1 and B_2 represent the multicenter bond orders).

7. References

- [1] M. J. Frisch. Gaussian 09, Revision D. 01 (Gaussian Inc., 2009).
- [2] A. D. Becke, *J. Chem. Phys.* 1993, 98, 5648-5652
- [3] P. J. Stephens; F. J. Devlin; C. F. Chabalowski; M. J. Frisch. *J. Phys. Chem.* 1994, 98, 11623-11627.
- [4] P. C. Hariharan; J. A. Pople, *Theor. Chim. Acta.* 1973, 28, 213-222.
- [5] J. W. Ochterski; G. A. Petersson ; J. A. Montgomery, *J. Chem. Phys.* 1996, 104, 2598-2619.
- [6] Q. Wang, Y. Shao and M. Lu, *Cryst. Growth Des.* 2018, 18, 6150-6154.
- [7] J. J. McKinnon, D. Jayatilaka and M. A. Spackman, *Chem. Commun.* 2007, 37, 3814-3816.
- [8] H. Huo, J. Zhang, J. Dong, L. Zhai, T. Guo, Z. Wang, F. Bi and B. Wang, *RSC advances.* 2020, 10, 11816-11822.
- [9] C. Li, T. Zhu, J. Tang, G. Yu, Y. Yang, H. Yang, C. Xiao, G. Cheng, *Chem. Eng. J.*

2024, 479, 147355.

[10] C. Li, T. Zhu, C. Lei, G. Cheng, C. Xiao, H. Yang, *J. Mater. Chem. A*. 2023, 11, 12043.

[11] T. Yan, J. Ma, H. Yang, G. Cheng, *Chem. Eng. J*, 2021, 429, 132416.